Journal of Geophysical Research: Earth Surface

Supporting Information for

Influence of Boulders on Channel Width and Slope: Field Data and Theory

Ron Nativ[1,2,3], Jens M. Turowski[3], Liran Goren[1], Jonathan B. Laronne[4] and J. Bruce H. Shyu[5]

[1]Department of Earth and Environmental Sciences, Ben-Gurion University of the Negev, Beer Sheva, 84105, Israel

[2]University of Potsdam, Institute of Earth and Environmental Science, Am Neuen Palais 10, 14469 Potsdam, Germany

[3]GeoForschungsZentrum, Helmholtz Centre Potsdam, Potsdam, Germany

[4]Department of Geography and Environmental Development, Ben-Gurion University of the Negev, Israel

[5]Department of Geosciences, National Taiwan University, Taipei, Taiwan

Correspondence to: Ron Nativ (ronnat@post.bgu.ac.il)

Contents of this file

Introduction

The following supporting information describes additional methods, calculations, and extended data analysis that aid this study.

Text S1: Error in Width Calculations

The field data width factor $Z = W_b/W$ includes various uncertainties, including (I) the error on the 3D model-derived orthophoto used to calculate the channel width. Based on one field location in the Liwu river where an orthophoto was compared to numerous measurements using a tape, this error is less than 20 cm and is thus very small in comparison to the actual channel width. (II) Uncertainty related to the channel reach being non-homogeneous in space. In other words, the measurement of a cross-section channel width is dependent on the location along the downstream direction. Here we assume that this is the most significant uncertainty. To calculate it, we utilize an error propagation technique according to the following. Assuming that uncertainties are normally distributed, the uncertainty ΔZ is given by

$$\Delta Z = \sqrt{\left(\frac{\Delta W}{W}\right)^2 + \left(\frac{\Delta W_b}{W_b}\right)^2} \quad \text{(S1)}$$

The boulder-bed and boulder-free widths, W_b and W, respectively, were derived using the methods described in the main text (Section 2). The error on the boulder-bed width ΔW_b was calculated as one standard deviation from the mean of 10 width measurements using a 3D model-derived orthophoto for each boulder-bed channel reach. In contrast, the boulder-free width ΔW was estimated using the maximal error on width derived from Google-earth imagery (Section 2 in the main text) and set a constant of $\Delta W = 0.2W$. With these, each boulder-bed channel width can be assigned with a specific error length.

Text S2: Comparison of Width Calculations Using Basin-scale Relationship and Direct Google-earth-derived Data

Boulder-concentration is generally smaller (~0.1) in smaller upstream reaches and shows large variability of 0 - 0.34 in larger drainage areas. Thus, the entire range of Γ is observed in drainage areas > 400 km^2. The two different approaches for calculating W yield relatively similar width ratios; 18 out of 20 are within 50% error relative to a one-to-one case (Fig. S1). Although the choice of 50% is somewhat arbitrary, the two marked outliers show a large discrepancy between the two applied approaches.

Text S3: Recurrence of Hillslope Failure Events in the Liwu River

The Liwu River forms a steep landscape with elevations drop of ~ 3000 m over a relatively short distance of 40 km (Fig. S1). Landslides, rockfalls, and debris-flows are three major hillslope transportation mechanisms that occur frequently—a few pieces of evidence of failure events that recurred at least two times are given as examples. The first location (24.171691, 121.551384) is a narrow and deep bedrock gorge incised into marble, located 1.5 km upstream of Swallow Grotto. The first of two documented events occurred on January 27th, 2016 (https://www.facebook.com/TarokoNationalPark/posts/1072687539455223/), while the second occurred on January 12th, 2021 (https://www.cna.com.tw/news/ahel/202101120033.aspx).

The second documented location (24.169664, 121.588059; see also reach number 17 in Table 2) is where a large landslide occurred between May, 2nd 2013 and May 9th, 2013. A snippet of the event from May 6th, 2013, was captured using a video camera (https://www.youtube.com/watch?v=ragw__sM2ac). The new forming slope can also be viewed in the following link (https://www.youtube.com/watch?v=ydL4-_YMjqA), where a controlled explosion partially evacuates the hillslope. Although we do not have direct media pieces of evidence for additional events in this specific location, an exploration of satellite imagery using the 'historical imagery' of Google Earth pro reveals that the adjacent downstream fluvial reach was already extensively covered with large boulders by 2006, implying a continuous supply of boulders.

Text S4: Testing the Horizontal Errors in Drone-Derived Three-Dimensional Models

To test the errors in boulder-concentration and boulder size analysis, we have performed the following study. A field locality was chosen in Baiyang (24.185005, 121.485815), a touristic trail with a concrete bridge crossing the tributary. Using a standard meter, we have measured by hand the length of seven objects with different lengths. Those objects included the bridge length, its width, and other observable shapes. Additionally, a drone was used to photograph the bridge vicinity using the same method described in Section 2.1. We followed the same procedure (section 2.1) to generate three-dimensional models, from which we generated an orthophoto. Then we measured the length of the same seven objects using the orthophoto and compared them to the lengths estimated by hand at the site. The comparison (Fig. S4) shows

that the lengths fall closely to a one-to-one reference line, indicating that our model includes minimal horizontal errors. The RMSE between model and observations is 6.5 cm.

Figures

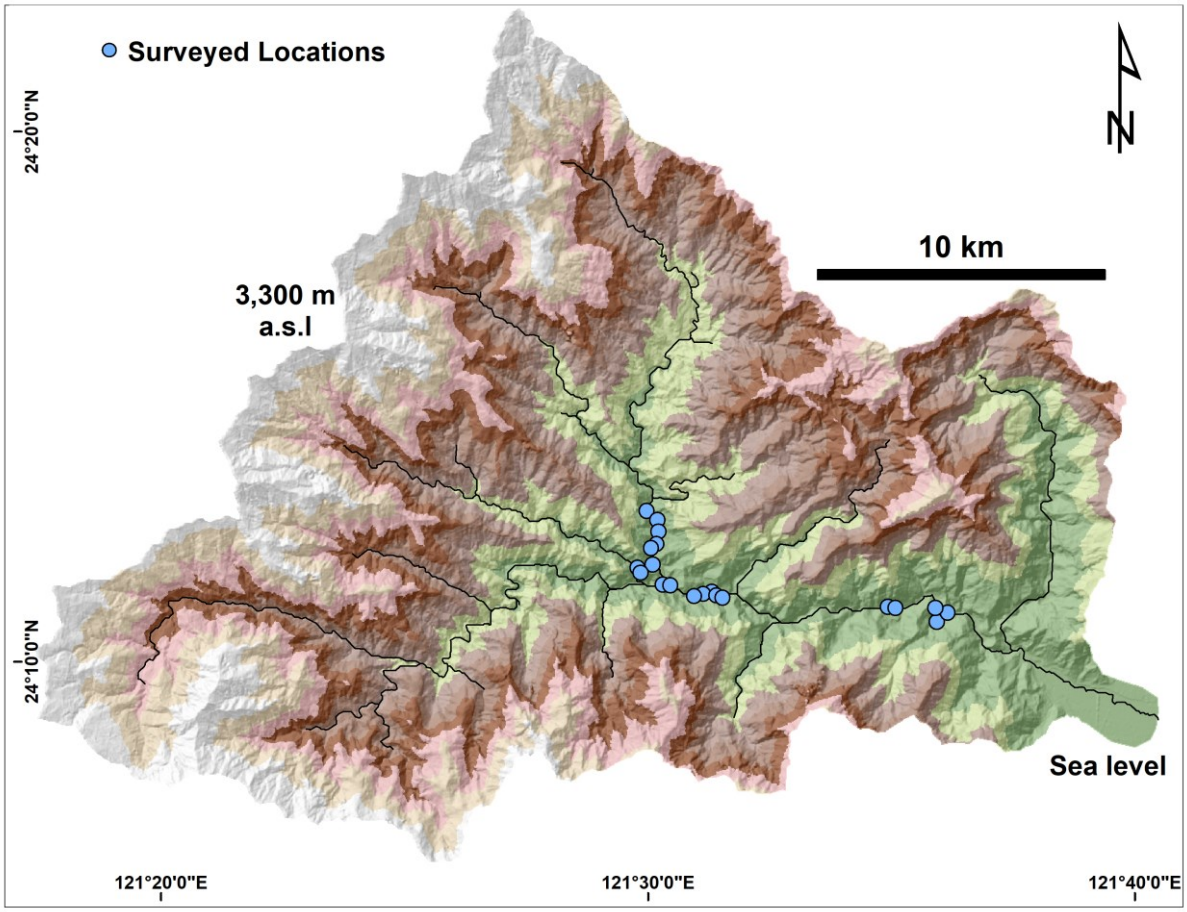

Figure S1: A 30 m DEM map of the Liwu River (630 km^2) overlain with the surveyed reach locations of boulder-bed channels in light blue circles. The location details are listed in Table 2 in the main text.

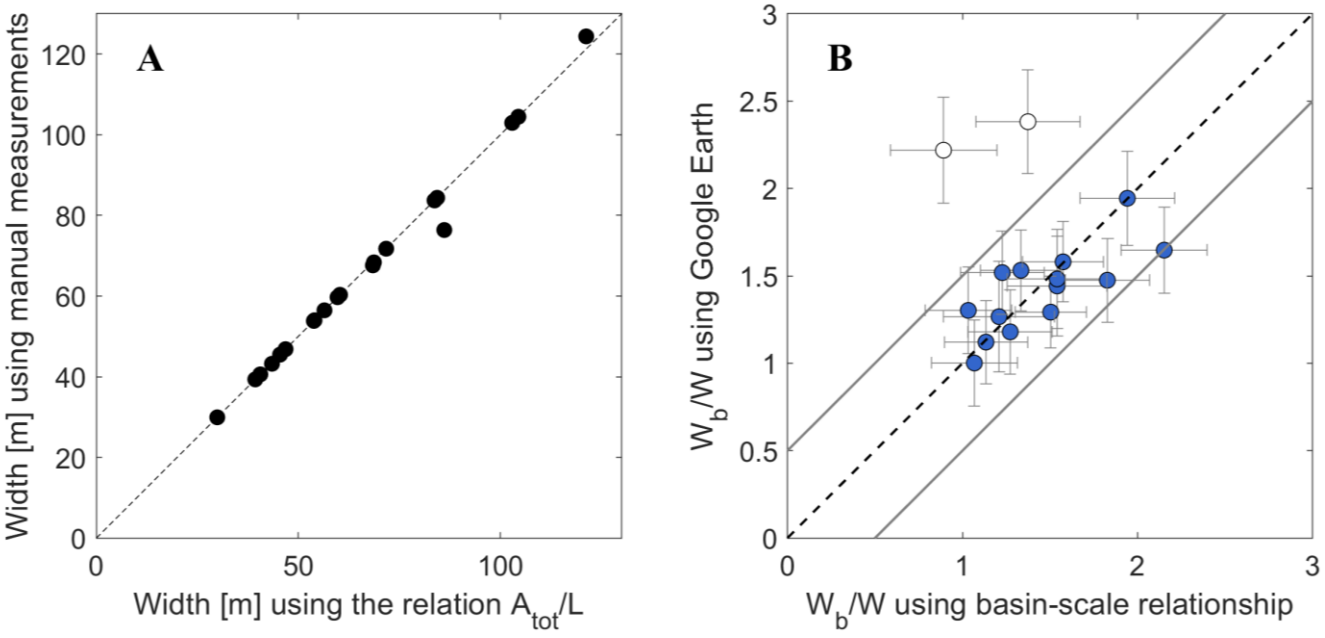

Figure S2: Comparison of two methods used to calculate channel width. The vertical axis shows channel width values calculated by dividing the channel reach area by the thalweg length, while the horizontal axis shows width values calculated using ten bank-to-bank lengths. The error bars on these values represents one standard deviation from the mean. The coefficient of correlation between the two data sets is $R^2 = 0.98$.

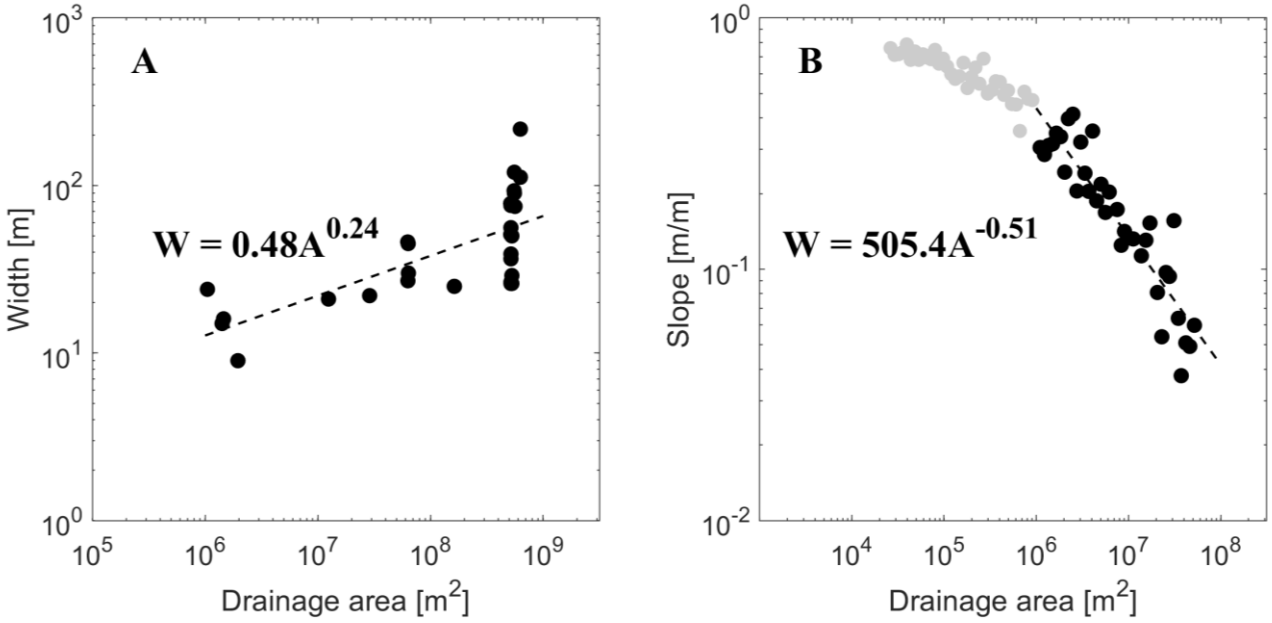

Figure S3: Channel morphology plotted versus drainage area for the Liwu river boulder-free channels. (A) Channel width of boulder-free tributaries increases with drainage area. A linear least mean squares on a log space yielded a power-law fit with R^2 = 0.49. (B) Channel slope of boulder-free tributaries decreases with drainage area. A linear least mean squares on a log space yielded a power-law fit with R^2 = 0.83. Channel width was measured in the field using a Laser Range Finder and by oserving minimal boulder presence. Channel slope was calculated using TopoToolBox, and segments with high concentrations of boulders were removed prior to the trend fit analysis.